Scaling Theory of Diblock Polyampholyte Solutions

4 AUTHORS, INCLUDING:

Nadya Shusharina
Massachusetts General Hospital

39 PUBLICATIONS **451** CITATIONS

SEE PROFILE

Ekaterina Zhulina
Institute of Macromolecular Compounds of t…

182 PUBLICATIONS **6,340** CITATIONS

SEE PROFILE

Andrey V Dobrynin
University of Akron

124 PUBLICATIONS **4,903** CITATIONS

SEE PROFILE

Scaling Theory of Diblock Polyampholyte Solutions

N. P. Shusharina,[†] E. B. Zhulina,[†,‡] A. V. Dobrynin,[§] and M. Rubinstein*[,†]

Department of Chemistry, University of North Carolina, Chapel Hill, North Carolina 27599-3290; Institute of Macromolecular Compounds of the Russian Academy of Science, 199004 St. Petersburg, Russia; and Polymer Program, Institute of Materials Science and Department of Physics, University of Connecticut, Storrs, Connecticut 26269-3136

Received June 22, 2005; Revised Manuscript Received August 8, 2005

ABSTRACT: We have developed a scaling theory for a salt-free solution of diblock polyampholytes. A charge-symmetric diblock polyampholyte chain with equally charged positive and negative blocks collapses into a globule. This collapse is driven by the electrostatic attraction between oppositely charged blocks. We predict that a charge-asymmetric block polyampholyte has a tadpole shape with a globular head and a polyelectrolyte tail. These tadpoles aggregate into micelles if the electrostatic repulsion between their tails is weaker than the surface energy gain due to aggregation of their heads. First tadpoles form double-tailed micelles. In double-tailed micelles with an aggregation number larger than two, additional chains are completely confined into the core, and the length of the two tails increases proportionally to the total charge of the micelle. If this total charge becomes higher than the charge of two corona blocks of double-tailed micelles, more blocks appear in the corona. Chains are disproportionated in all micelles. They are divided into two populations: chains in one group are completely confined inside the micellar core, while the other group of chains has an entire block placed in the corona. Micelles with disproportionated chains remain stable even if the net charge of a block polyampholyte is as small as one elementary charge per chain. This stability is due to (i) a long corona consisting of entire stronger charged blocks and (ii) weaker charged blocks in the core are not stretched because of the presence of entire diblock chains confined in the core.

1. Introduction

For several decades, charged polymers remain an important subject in polymer science.[1−4] There are two different classes of charged polymers: polyelectrolytes and polyampholytes. Polyelectrolytes are polymers containing either basic or acidic groups. Examples of polyelectrolytes include DNA, poly(methacrylic acid), and poly(2-(dimethylamino)ethyl methacrylate). Polyampholyte chains differ from polyelectrolytes because they contain both acidic and basic groups.[3] For example, in proteins, positive and negative charges are distributed in a very specific manner along the polymer backbone. In synthetic polyampholytes, charge sequence is typically random while the fraction of positively and negatively charged groups can be adjusted by monomer concentration during polymerization reaction. Also, the degree of blockiness can be modified by changing the reactivity ratios. This control over the charge distribution along the polymer backbone allows one to generate random or regular (blocklike) sequences of ionic groups. The properties of polyampholyte solutions are strongly coupled with their chemical structure.[5,6] The fraction of positively and negatively charged groups can be fixed (strong polyampholytes), or it can be dependent on solution pH (weak polyampholytes). In the present paper we will consider the former case of quenched charges; nevertheless, our theory can be applied to the latter case of annealed charges if the solution pH is fixed and one ignores the effect of local electrostatic potential on the pK of the charged groups. It was shown[5] that polymer solubility depends on the uncompensated (net) charge of polyampholytes and on the sequence of posi-

tive and negative charges along the chain. Random polyampholytes become less soluble with decreasing net charge. The properties of block polyampholytes in solution are expected to be quite different from those of random polyampholytes. Block charge sequences allow formation of large molecular aggregates of a well-defined size−micelles. Recent experimental studies of solutions of block polyampholytes[7,8] have shown that these polymers form micelles in a wide range of solution pH on both sides of the isoelectric point. These unique properties of polyampholytes find applications in water purification, colloidal stabilization, and drug delivery.

A theoretical model of aggregation in solutions of block polyampholytes was recently proposed by Castelnovo and Joanny.[9] They studied the solution phase diagram at high ionic strengths and determined the phase boundary and the critical micelle concentration as functions of polymer concentration and net charge of the chains. The size of these micelles and their aggregation number was found to be a strong function of the fraction of charged monomers on the polymer backbone. The micellar core in this model[9] was assumed to be formed by weaker charged blocks and the compensating fraction of stronger charged blocks, so that the net charge of the core is very close to zero. The core structure of the aggregate is similar to the structure of the solution of oppositely charged polyelectrolytes considered in refs 10 and 11. The formalism developed in refs 10 and 11 is based on RPA approximation and accounts for charge density fluctuations in homogeneous solution. Since the local structure of the core of the micelle is similar to that in the solutions of oppositely charged polyelectrolytes, one can use RPA formalism developed in refs 10 and 11 to describe polymer and charge density fluctuations inside micellar core. This approximation is valid as long as the characteristic

[†] University of North Carolina.
[‡] Institute of Macromolecular Compounds of the Russian Academy of Science.
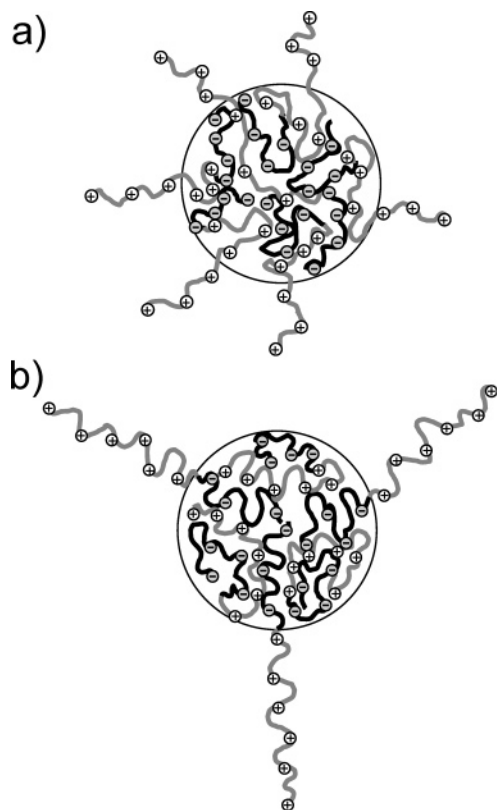[§] University of Connecticut.

Figure 1. Schematic sketch of individual micelles: (a) starlike micelle according to the restricted model; (b) starlike micelle with disproportionated chains according to the unrestricted model.

length scale of fluctuations is much smaller than the size of the micellar core. The corona of the block polyampholyte micelles within the model proposed by Castelnovo and Joanny[9] is formed by charge-unbalanced sections of blocks with higher net charge (see Figure 1a). The structure of such micelles is, therefore, similar to the structure of micelles made of diblock copolymers with one hydrophobic and one polyelectrolyte block. The main difference is that in the polyampholyte micelles both blocks participate in the formation of the core, and the corona consists not of the entire higher charged block but only of a part of it (Figure 1a).

In the present paper we propose that polyampholyte micelles can have a structure qualitatively different from that considered by Castelnovo and Joanny.[9] The charge compensation in the core of the micelle is achieved by confining all blocks carrying the smaller charge and a compensating number of entire blocks carrying the larger charge (see Figure 1b). The partitioning (disproportionation) of blocks carrying a charge of the same sign between the core and the corona of the micelle leads to a lower micellar free energy per chain which changes the critical micelle concentration, the aggregation number, and significantly improves micellar stability. Such disproportionation of polyampholyte chains has been observed in the lattice mean field theory studies and Monte Carlo simulations of polyampholyte brushes in both planar[12] and spherical[13] geometries.

The disproportionation of chains in the systems containing oppositely charged polyelectrolytes has been recently predicted by Zhang and Shklovskii.[14] If the total positive charge carried by polymers is not equal to the total negative charge, the polyelectrolyte complexes made of a long polyanion and shorter polycations

are charged and have a tadpole conformation. If the ratio of the total charge of polyanions and polycations is close to unity, the solution phase separates into a neutral sediment and a supernatant of stronger charged tadpoles and counterions.

Below we will consider micelles formed in solutions of block polyampholytes at low salt concentrations by adopting the model with block disproportionation between the core and corona of the micelle. Our scaling model predicts that any charge asymmetry (even the difference of one elementary charge) is sufficient to stabilize micelles formed by monodisperse block polyampholytes. The rest of the paper is organized as follows. We will describe our theoretical model and apply it to determine the conformations of a single chain in section 2 and the structure of micelles of diblock polyampholytes in section 3. The discussion and conclusions are presented in section 4.

2. Conformations of a Block Polyampholyte Chain

Consider a diblock polyampholyte with degree of polymerization $N = N_+ + N_-$ (N_+ monomers in a positively charged block and N_- monomers in a negatively charged block) in a polar solvent (e.g., in water) of dielectric permittivity ϵ at temperature T. Both blocks are assumed to be flexible polymers with the same Kuhn length b. The nonelectrostatic interactions of monomers with the solvent are θ-like; i.e., the first nonzero term in the virial expansion of the monomer interaction energy corresponds to the three-body repulsion. The generalization of the theory to the good solvent condition is straightforward, and the results are presented in Table 2. The fraction of charged monomers is assumed to be the same for both blocks, $f_+ = f_- = f$. The block asymmetry $\Delta N = N_+ - N_-$ is therefore a measure of the net chain charge eZ_{net}

$$eZ_{net} \equiv e\Delta Nf \qquad (1)$$

where e is the elementary charge and Z_{net} is the net valence of the diblock.

2.1. High Charge Asymmetry. Conformations of polyampholyte chains at high charge asymmetry $\Delta N \sim N$ are similar to those of polyelectrolyte chains. The intrachain electrostatic interactions lead to elongation of a polyelectrolyte chain in dilute solutions into an array of electrostatic blobs.[15,16] The size of an electrostatic blob, ξ_{el}, is determined by the condition that the energy of electrostatic interaction of two neighboring blobs along the chain is equal to the thermal energy:

$$\frac{e^2 f^2 g_{el}{}^2}{\epsilon \xi_{el}} \approx k_B T \qquad (2)$$

where g_{el} is the number of monomers in a blob, ϵ is the solvent dielectric constant, k_B is the Boltzmann constant, and T is the absolute temperature. (We keep our discussion in the present paper at the level of scaling approximation and omit numerical prefactors and logarithmic corrections except for section 3.1.) Taking into account Gaussian statistics of a chain in a θ-solvent on the length scale smaller than the electrostatic blob size ($\xi_{el} \approx bg_{el}{}^{1/2}$), one obtains the size of the electrostatic blob:
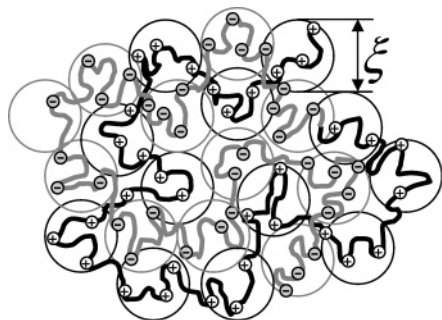
$$\xi_{el} \approx b(uf^2)^{-1/3} \qquad (3)$$

Figure 2. Blob picture of a polyampholyte globule is similar to a concentrated solution of oppositely charged polyelectrolytes. A correlation volume (blob) containing a section of a positively charged chain is surrounded by blobs containing sections of negatively charged chains. $\xi \approx \xi_{el}$ is the correlation blob size.

where $u \equiv l_B/b$ is the ratio of the Bjerrum length

$$l_B = \frac{e^2}{\epsilon k_B T} \qquad (4)$$

to the Kuhn length b.

The energy of a polyelectrolyte in the elongated conformation is on the order of the thermal energy $k_B T$ per electrostatic blob

$$\frac{F_{polyel}}{k_B T} \approx \frac{N}{g_{el}} \approx N(uf^2)^{2/3} \qquad (5)$$

2.2. Charge-Symmetric Case. In the case of charge-symmetric polyampholytes, $\Delta N = 0$, strong intrachain attractive interactions due to charge density fluctuations[10,11] lead to a collapse of the polyampholyte diblock into a globule (Figure 2). The equilibrium density of a globule is determined by the balance between fluctuation-induced attraction and three-body repulsion (in the case of a θ-solvent). Inside the globule there is an important length scale called the correlation length ξ. Polymer statistics at the length scale smaller than the correlation length is unperturbed by the fluctuation-induced attractive interactions leading to the usual for a θ-solvent scaling relation between the correlation length ξ and the number of monomers g in the correlation blob, $\xi \approx bg^{1/2}$. At the length scales larger than the correlation length, the attractive interactions cause dense packing of the correlation blobs. The local structure of the melt of blobs resembles that of a concentrated solution of positively and negatively charged polyelectrolytes with each blob being surrounded by the oppositely charged blobs with high probability (see Figure 2). The electrostatic interactions between any two neighboring blobs are on the order of the thermal energy $k_B T$:

$$k_B T \left| \frac{l_B f^2 g^2}{\xi} \right| \approx k_B T \qquad (6)$$

The blob size, ξ, is, therefore, determined by the condition similar to that controlling the size of an electrostatic blob (see eq 2). However, in the case of symmetric polyampholytes, two neighboring blobs are oppositely charged, reflecting the attractive nature of the intrachain interactions. Qualitatively, the typical length scale of the repulsive electrostatic interactions in strongly charge-asymmetric block polyampholyte

chains (eq 3) is the length scale of the attractive interactions in charge-symmetric polyampholytes.

$$\xi \approx \xi_{el} \qquad (7)$$

The correlation blobs inside the globule are space filling leading to the following expression for the local monomer concentration

$$c_{gl} \approx \frac{g}{\xi^3} \approx \frac{1}{b^2\xi} \approx \frac{1}{b^3}(uf^2)^{1/3} \qquad (8)$$

The size of a globule of a charge-symmetric diblock polyampholyte is

$$R_{gl} \approx (N/c_{gl})^{1/3} \approx bN^{1/3}(uf^2)^{-1/9} \qquad (9)$$

Each blob inside the globule is attracted to a neighboring oppositely charged blob with the energy on the order of the thermal energy $k_B T$. Thus, in the framework of the scaling approach we can estimate the bulk contribution to the free energy of a globule proportional to the number of blobs in the globule

$$\frac{F_{gl}}{k_B T} = -\frac{N}{g} \approx -\frac{Nb^2}{\xi^2} \approx -N(uf^2)^{2/3} \qquad (10)$$

This free energy is on the same order of magnitude as the electrostatic energy of a polyelectrolyte chain (eq 5), and the minus sign reflects the attractive nature of the intrachain interactions.

In addition to the bulk free energy, a polyampholyte globule has a surface free energy contribution due to the polymer−solvent interface. The origin of this term is the difference between the number of nearest neighbors of a blob inside the globule and on the globular surface. The surface energy can be estimated as the thermal energy $k_B T$ per each correlation blob on the surface of the globule:[17]

$$\frac{F_{surf}}{k_B T} \approx \frac{R_{gl}^2}{\xi^2} \approx N^{2/3}(uf^2)^{4/9} \qquad (11)$$

The electrostatic interactions are weak in comparison with the thermal energy $k_B T$ at very low fraction f of charged monomers along the polymer. In this case, the chain is in a coil state with the size $R \approx bN^{1/2}$ almost unperturbed by the interactions. The crossover to a globule in the case of charge-symmetric block polyampholytes or to an elongated chain in the strongly charge-asymmetric case occurs when there is more than one electrostatic blob per chain (the energy of the electrostatic interactions is larger than the thermal energy $k_B T$). The electrostatic blob size (eq 3) is on the order of the Gaussian size of a diblock polyampholyte $bN^{1/2}$ at

$$N_{neutr} \approx (uf^2)^{-2/3} \qquad (12)$$

or at the fraction of charged monomers

$$f_{neutr} \approx N^{-3/4}u^{-1/2} \qquad (13)$$

Below this fraction of charged monomers (for $f < f_{neutr}$) the conformations of a diblock polyampholyte are not affected by the electrostatic interactions. This boundary is shown by a vertical solid line in the diagram in Figure 3.
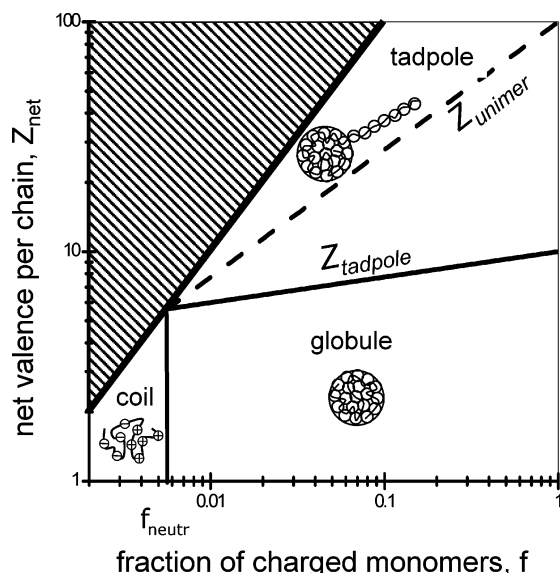
Figure 3. Diagram of states of a diblock polyampholyte in the fraction of charged monomers, $f_+ = f_- = f$, and the net valence per chain, Z_{net}, plane calculated for $N = 1000$, $u = 1$ (logarithmic scales). The shaded area indicates the inaccessible range of parameters.
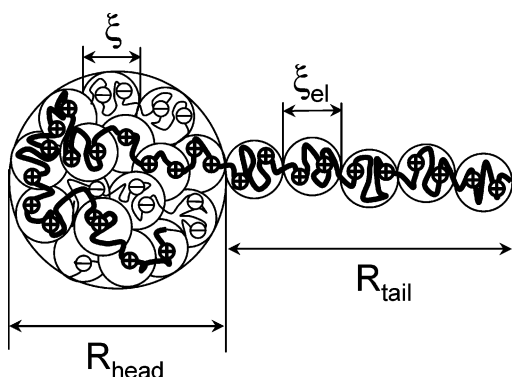

Figure 4. Schematic sketch of a tadpole conformation of a unimer with head size R_{head} and tail length R_{tail}.

2.3. Intermediate Charge Asymmetry. At the intermediate charge asymmetries ($g_{el} \ll \Delta N \ll N$) a block polyampholyte chain forms a tadpole (see Figure 4) with the head size R_{head} and the tail length R_{tail}. The analysis of the monomer chemical potential presented in Appendix shows that the partitioning of charged monomers between the head and the tail is determined by the balance of the charge density fluctuation-induced attractive interactions inside the head (energy gain per monomer for bringing an extra charged chain section into the head) and work per monomer done against Coulomb repulsion upon bringing an extra charge into the head. This condition for the partitioning of monomers between the head and the tail of the tadpole can be rewritten in terms of the reduced electrostatic potentials of the head and of the tail

$$\frac{l_B Z_{head}}{R_{head}} \approx \frac{l_B Z_{tail}}{R_{tail}} \qquad (14)$$

where eZ_{head} and eZ_{tail} are the charges of the head and the tail, and R_{head} and R_{tail} are the size of the head and the length of the tail, respectively. The size of the head is approximately equal to the size of the globule (eq 9) since most of the monomers are in the head ($\Delta N \ll N$).

The right-hand side of eq 14 is proportional to the linear charge density of the tail $g_{el}f/\xi_{el} \sim \xi_{el}f/b^2 \sim f(uf^2)^{-1/3}/b$. Thus, the valence of the head is on the order of

$$Z_{head} \approx \frac{R_{head}}{b}f(uf^2)^{-1/3} \qquad (15)$$

The valence of the head can be estimated by substituting eq 9 for the head size into eq 15

$$Z_{head} \approx N^{1/3}f(uf^2)^{-4/9} \approx Nf\left(\frac{N_{neutr}}{N}\right)^{2/3} \qquad (16)$$

The charge of the tadpole head eZ_{head} is much smaller than the charge of the block that is completely in the head eN_-f.

Relation 14 defines the relative partitioning of charge between the two parts of the diblock polyampholyte: the head and the tail of the tadpole. As the length of the tail exceeds the head size, the valence of the tail becomes larger than the net valence of the head Z_{head}. Thus, there are two different scaling regimes depending on the block charge asymmetry. The first regime corresponds to a unimer with a relatively large head and a tail with a length much smaller than the head size. On the scaling level, the tail in this regime is invisible, and the overall shape of the chain approximately resembles a polyampholyte globule. In the second regime the tail is very long in comparison with the size of the head, and its charge is much larger than that of the head. A polyampholyte chain in this regime can be thought of as a polyelectrolyte chain with a small head carrying a negligible charge, but the mass of the head could still be much larger than that of the tail. We will call the chains with such shape tadpoles.

The length of the tadpole tail is estimated as $R_{tail} \approx \xi_{el}\Delta N/g_{el}$, and using eq 3, we get

$$R_{tail} \approx b\Delta N(uf^2)^{1/3} \qquad (17)$$

The crossover between the regimes of globules and tadpoles occurs when $R_{head} \approx R_{tail}$ (cf. eqs 9 and 17), leading to the net valence per chain equal to

$$Z_{tadpole} \approx N^{1/3}f(uf^2)^{-4/9} \approx Nf\left(\frac{N_{neutr}}{N}\right)^{2/3} \qquad (18)$$

which is on the same order of magnitude as the valence of the head (eq 16). This crossover is shown by a solid line in Figure 3.

In dilute solutions the free energy of a polyampholyte chain can be written as the sum of the following contributions:

$$F_{unimer} = F_{head} + F_{tail} + k_B T Z_{net} \ln\left(Z_{net}\frac{c}{N}\right) + k_B T \ln\left(\frac{c}{N}\right) \qquad (19)$$

The first term in eq 19 is the energy of the head consisting of the energy of fluctuation-induced attraction $F_{gl} \approx -k_B TN/N_{neutr}$ (eq 10), surface free energy $F_{surf} \approx k_B T(N/N_{neutr})^{2/3}$ (eq 11), and the electrostatic self-energy

$$\frac{F_{el}^{head}}{k_B T} \approx \frac{l_B Z_{head}^2}{R_{head}} \approx N^{1/3}(uf^2)^{2/9} \approx \left(\frac{N}{N_{neutr}}\right)^{1/3} \qquad (20)$$

The second term in eq 19 is the electrostatic self-energy of the tail

$$\frac{F_{el}^{tail}}{k_B T} \approx \frac{l_B Z_{tail}^2}{R_{tail}} \approx \Delta N (uf^2)^{2/3} \approx \frac{\Delta N}{N_{neutr}} \qquad (21)$$

The last two terms in eq 19 are the entropy of the counterions and of the chains in the solution, respectively.

The crossover from the regime of tadpoles to the regime of polyelectrolyte chains occurs at $\Delta N \approx N$. The thick solid line in Figure 3 represents the upper boundary of the diagram $Z_{net} = Nf$. The shaded area above this line corresponds to the inaccessible range of parameters for the chosen degree of polymerization $N = 1000$.

In the next section we will consider micellization in dilute polyampholyte solutions and discuss how net charge per chain influences micellar structure.

3. Block Polyampholyte Micelles

The aggregation in solutions of block polyampholytes is driven by the charge density fluctuation-induced attractive interactions between oppositely charged blocks. By bringing two molecules together, one reduces the energy of the polymer−solvent interface and optimizes the free energy contribution due to the fluctuation-induced attraction. The stabilizing factor which prevents the formation of an infinite aggregate with increasing polymer concentration is the electrostatic repulsion between polyampholyte molecules if they carry the net uncompensated charge eZ_{net}. The optimal aggregation number of micelles is achieved according to the detailed balance between the surface energy and the electrostatic repulsion between chains due to their net charge.

Note that micelles can form when the surface energy of the head (eq 11) is larger than the electrostatic energy of the tail (eq 21), i.e., when the net valence is smaller than

$$Z_{unimer} \approx N^{2/3} f (uf^2)^{-2/9} \approx Nf \left(\frac{N_{neutr}}{N}\right)^{1/3} \qquad (22)$$

In the opposite case, $Z_{net} > Z_{unimer}$, unimers are stable because bringing two polyampholyte molecules together leads to the increase of electrostatic repulsion larger than the decrease in the surface energy of the aggregate. This crossover is shown by the dashed line in Figure 3.

Below we analyze the structure of micelles and calculate their equilibrium aggregation number, i.e., the number of individual chains forming a micellar aggregate, p, as a function of the charge fraction of the blocks, f, and the net charge per chain, eZ_{net}.

3.1. Double-Tailed Micelles. Below the crossover boundary given by eq 22 (for $Z_{net} < Z_{unimer}$) the surface energy of the tadpole head becomes larger than the electrostatic energy of the tail, the energetic requirement for micellization is fulfilled, and unimers start to aggregate above the critical micelle concentration. Two tadpole unimers form a dimer with a common head and two tails sticking out of the head in opposite directions (see Figure 5a). The larger p-mers can be formed in two alternative ways. One possible structure is realized when the total net charge of the micelle

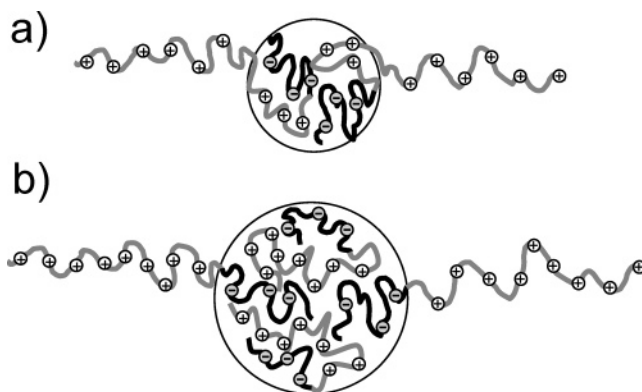$$eZ_{mic} = epZ_{net} \qquad (23)$$

Figure 5. Schematic sketch of (a) a dimer and (b) a double-tailed micelle.

is carried by p equivalent tails in the corona (see Figure 1a). All chains in such micelle are in a similar conformation contributing the same portion of the longer block to the core of the micelle. We will call such arrangement of polyampholyte chains in the micelle the *restricted model*. In the *unrestricted model* one releases the equipartition constraint, allowing some chains to be completely confined in the core of the micelle while the two tails increase in length proportionally to the increase of the aggregate's net charge. The resulting micelle has a large head with the two tails in the corona (Figure 5b). Such structure is similar to the one of the dimer, but in the case of a larger double-tailed micelle the head contains $p - 2$ chains completely confined in it and two partially confined ones.

To compare the two models, we calculate the electrostatic energy associated with the total charge eZ_{mic} of the aggregate. In the case of long corona chains the electrostatic energy per chain is equal to

$$\frac{F_{el}^{corona}}{k_B T} \approx \frac{l_B Z_{mic}^2}{p R_{corona}} \approx \frac{l_B p Z_{net}^2}{R_{corona}} \qquad (24)$$

The corona size R_{corona} in the restricted model is calculated by balancing the energy of electrostatic repulsion with the elastic energy of the sections of blocks, ΔN, forming the corona

$$\frac{F_{str}^{restr}}{k_B T} \approx \frac{R_{corona}^2}{\Delta N b^2} \qquad (25)$$

From eqs 24 and 25 the corona size in the restricted model is estimated as

$$R_{corona}^{restr} \approx b p^{1/3} \Delta N (uf^2)^{1/3} \qquad (26)$$

Substituting eq 26 into eq 24, we obtain the corona free energy per chain for the restricted model

$$\frac{F_{el}^{restr}}{k_B T} \approx p^{2/3} \Delta N (uf^2)^{2/3} \approx p^{2/3} \frac{\Delta N}{N_{neutr}} \qquad (27)$$

Given the approximation of a double-tailed micelle with tails containing $p\Delta N$ monomers (which is much larger than the head), the charge of the micelle is stored mostly in the tails and their linear size is on the order of (cf. eq 17)

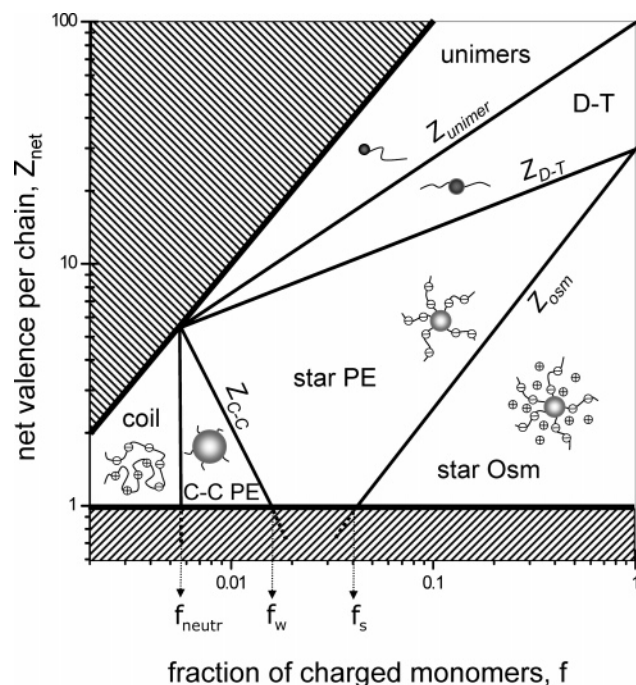$$R_{tail} \approx b p \Delta N (uf^2)^{1/3} \qquad (28)$$

Figure 6. Diagram of different regimes for the diblock polyampholyte micelles in a fraction of charged monomers, f, and net valence per chain, Z_{net}, plane calculated for $N = 1000$, $u = 1$ (logarithmic scales). The shaded area indicates the inaccessible range of parameters.

The electrostatic energy per chain in a double-tailed micelle is

$$\frac{F_{\text{el}}^{\text{D-T}}}{k_{\text{B}}T} \approx \Delta N(uf^2)^{2/3} \approx \frac{\Delta N}{N_{\text{neutr}}} \qquad (29)$$

The cores of the micelles with the same aggregation number in the two models have the same energy; therefore, comparing the electrostatic energies of the coronas (eqs 27 and 29), one can see that the free energy of a micelle in the unrestricted model (eq 29) is lower than that in the restricted model (eq 27). Thus, we conclude that micelles with disproportionated chains are more favorable than the ones with all the chains having the same fraction of longer blocks in the corona.

The diagram in Figure 6 shows the regimes of different structures of micelles with disproportionated chains depending on the fraction of charged monomers, f, and the net valence per chain, Z_{net}. The unshaded area corresponds to the range of experimentally accessible parameters. The double-tailed micelle regime is denoted in the diagram by "D−T".

The surface energy per chain of the micelle formed by p polyampholyte chains with the core radius (cf. eq 9)

$$R_{\text{core}} \approx bp^{1/3}N^{1/3}(uf^2)^{-1/9} \qquad (30)$$

is given by

$$\frac{F_{\text{surf}}}{k_{\text{B}}T} \approx \frac{R_{\text{core}}^2}{p\xi^2} \approx p^{-1/3}N^{2/3}(uf^2)^{4/9} \qquad (31)$$

The electrostatic energy per chain of the double-tailed micelle (eq 29) does not depend on the aggregation number p. Indeed, to estimate the size of an

equilibrium double-tailed micelle, we have to introduce a logarithmic correction to the electrostatic self-energy of the tails:

$$\frac{F_{\text{el}}^{\text{tail}}}{k_{\text{B}}T} \approx \Delta N(uf^2)^{2/3} \ln(p\Delta N(uf^2)^{2/3}) \qquad (32)$$

Minimization of the electrostatic energy per chain in the corona of a micelle and the core surface energy per chain (eq 31) with respect to the micellar aggregation number p results in the equilibrium aggregation number of double-tailed micelles

$$p_{\text{D-T}} \approx \frac{N^2 f^3}{Z_{\text{net}}^3}(uf^2)^{-2/3} \approx \frac{(Nf)^3}{Z_{\text{net}}^3}\frac{N_{\text{neutr}}}{N} \qquad (33)$$

The crossover between double-tailed micelles and isolated chains − unimers − in the tadpole conformation (eq 22) occurs when the micellar aggregation number (eq 33) is equal to unity.

Note that the logarithmic correction in eq 32 justifies lower electrostatic energy of the double-tailed conformation with respect to the single-tail conformation of the micelle. However, this weak logarithmic dependence allows for strong fluctuations in lengths of the tails or, equivalently, in position of the micellar core.

The aggregation number of double-tailed micelles (eq 33) increases with decreasing net charge of a chain eZ_{net}, and eventually the net charge of the micelle, eZ_{mic}, becomes equal to the charge of the two longer blocks eN_+f. This takes place at the crossover boundary (see Figure 6)

$$Z_{\text{D-T}} \approx N^{1/2}f(uf^2)^{-1/3} \approx Nf\left(\frac{N_{\text{neutr}}}{N}\right)^{1/2} \qquad (34)$$

Below this boundary (for $Z_{\text{net}} < Z_{\text{D-T}}$) the corona of the micelle consists of more than two chains corresponding to the regime of starlike polyelectrolyte micelles.

3.2. Starlike Micelles. Micelles with corona thickness much larger than the radius of the core are referred to as starlike or hairy. In this case the charge eZ_{mic} is located mostly in the micellar corona.

Each disproportionated micelle in the unrestricted model is composed of p chains with p' positively charged blocks completely in the corona and $p - p'$ chains completely confined in the core (see Figure 1b). The charge balance in the core

$$pN_- \approx (p - p')N_+ \qquad (35)$$

gives an estimate for the number of positively charged blocks in the corona of the micelle p'

$$p' \approx 2p\frac{\Delta N}{N + \Delta N} \approx p\frac{Z_{\text{net}}}{Nf} \qquad (36)$$

The equilibrium aggregation number of these micelles is determined by the balance of the surface energy of the core (eq 31) and the electrostatic energy of the corona with the total charge eZ_{mic}. This energy is calculated by assuming that the counterions are redistributed between the micelle and the surrounding solution; i.e., the fraction α of them is freely floating in the solution, and the fraction $1 - \alpha$ is condensed in the micelle reducing its charge.[18] (By condensation we mean that the counterions are localized either inside the

micelle or within the distance on the order of micellar radius, R_{mic}, of its surface.)

The electrostatic energy per chain of a starlike micelle with the effective charge $e\alpha pZ_{net}$ is

$$\frac{F_{el}^{mic}}{k_B T} \approx \frac{pZ_{net}^2 \alpha^2 l_B}{R_{mic}} \quad (37)$$

and the entropic part of the free energy per chain due to counterions is

$$\frac{F_{count}}{k_B T} \approx Z_{net}(1-\alpha) \ln\left(\frac{Z_{mic}(1-\alpha)}{R_{mic}^3}\right) + Z_{net}\alpha \ln\left(Z_{net}\frac{c}{N}\alpha\right) \quad (38)$$

where eZ_{net} is the net charge of a chain, $eZ_{mic} = epZ_{net}$ is the net charge of a micelle, the size of the micelle is the sum of that of a core and of a corona

$$R_{mic} = R_{core} + R_{corona} \quad (39)$$

and c is the average monomer concentration in the solution. The two terms in eq 38 are the entropic part of the free energy per chain due to condensed and free counterions, respectively.

Star Polyelectrolyte Regime ($\alpha \sim 1$). We consider two limiting cases with respect to the value of the parameter α. The limit $\alpha \sim 1$ corresponds to the situation with most of the counterions in the surrounding solution and with micellar charge remaining practically unscreened. The counterions can be considered as free if the electrostatic potential at the outer edge of the micelle (the interaction energy of a probe elementary charge e with the micelle) is smaller than the thermal energy $k_B T$:

$$\frac{Z_{mic}l_B}{R_{mic}} < 1 \quad (40)$$

i.e., if the entropy loss due to confinement of a counterion inside the micelle is larger than the energy gain due to the reduction of the electrostatic repulsion. We will call this case the star polyelectrolyte regime and denote it by "star PE" in the diagram in Figure 6.

The interactions between corona chains are purely electrostatic, and the equilibrium size of the corona is determined by the balance of the energy of electrostatic repulsion between chains in the corona (eq 24) and their elastic energy due to stretching to the corona size R_{corona}. In the case of starlike micelles most of the micellar volume is occupied by the corona ($R_{mic} \approx R_{corona}$). The number of monomers in each of the corona blocks is $N_+ = N(1 + \Delta N/N)/2 \approx N$. The elastic energy of a starlike micelle per chain (cf. eq 25)

$$\frac{F_{str}}{k_B T} \approx \frac{p'}{p}\frac{R_{corona}^2}{N_- b^2} \approx \frac{p'}{p}\frac{R_{corona}^2}{Nb^2} \quad (41)$$

is equilibrated by the electrostatic energy (eq 24) leading to the optimum size of the corona

$$R_{corona} \approx bp^{1/3}N\left(\frac{\Delta N}{N}\right)^{1/3}(uf^2)^{1/3} \quad (42)$$

Note that, the corona size, R_{corona}, of a disproportionated

micelle given by eq 42 is larger than that in the restricted model (see eq 26). Therefore, the same net charge, eZ_{mic}, is placed in the unrestricted model on fewer but longer chain sections in the corona which makes the electrostatic energy of the disproportionated micelle lower than the electrostatic energy in the restricted model.

The corona size R_{corona} is larger than the length of an individual (free) polyelectrolyte block (see eq 17) because of the additional stretching of the blocks in the corona caused by interchain electrostatic repulsion. Each block in the corona can be represented as a sequence of tension blobs[17] with size:

$$\xi_t \approx \frac{b^2 N}{R_{corona}} \approx b\left(p\frac{\Delta N}{N}\right)^{-1/3}(uf^2)^{-1/3} = \frac{\xi_{el}}{\left(p\frac{\Delta N}{N}\right)^{1/3}} \quad (43)$$

The size of a tension blob is equal to the electrostatic blob size at the Z_{D-T} crossover line ($p\Delta N/N \approx 1$) between double-tailed and starlike micelles. Substituting eq 42 into the expression for the electrostatic energy of the corona (eq 24), we obtain the electrostatic contribution to the total energy of the micelle per chain in the unrestricted model with the disproportionation of the chains:

$$\frac{F_{el}^{corona}}{k_B T} \approx p^{2/3}N\left(\frac{\Delta N}{N}\right)^{5/3}(uf^2)^{2/3} \quad (44)$$

This energy is lower than that of the corona electrostatic energy in the restricted model (cf. eq 27).

The aggregation number in the polyelectrolyte regime of the unrestricted model is determined by the balance of the electrostatic free energy of the corona (eq 44) and surface free energy of the core (eq 31):

$$p_{PE} \approx \frac{1}{N^{1/3}\left(\frac{\Delta N}{N}\right)^{5/3}}(uf^2)^{-2/9} \approx \frac{(Nf)^{5/3}}{Z_{net}^{5/3}}\left(\frac{N_{neutr}}{N}\right)^{1/3} \quad (45)$$

Osmotic Regime ($\alpha \ll 1$). Another limiting case of eq 37 is achieved when most of the counterions are condensed on the micelles $\alpha \ll 1$, resulting in stretching of chains in the corona stabilized by osmotic force due to entropy of the confined counterions. We refer to this regime as osmotic and denote it in the diagram shown in Figure 6 by "star Osm".

At the crossover between osmotic and polyelectrolyte regimes the electrostatic potential at the edge of a micelle is on the order of the thermal energy $k_B T$ (up to logarithmic corrections):

$$\frac{Z_{mic}l_B}{R_{mic}} \approx 1 \quad (46)$$

For this value of the electrostatic potential the tension blob size, ξ_t (eq 43), is equal to the distance between charges along the polymer backbone. Thus, the free energy loss due to block stretching is on the order of thermal energy $k_B T$ per charge, i.e., the same as the entropy gain per counterion released from the corona. At this point excess counterions start condensing on the micelles screening electrostatic repulsion between uncompensated charges.

The stretching force in the osmotic regime is dominated by the entropy of the confined counterions (eq 38 at $\alpha \ll 1$); it is usually referred to as the osmotic contribution to the free energy of the micelle.

$$\frac{F_{\text{osm}}}{k_{\text{B}}T} \approx Z_{\text{net}} \ln\left(\frac{Z_{\text{mic}}b^3}{R_{\text{corona}}^{\,3}}\right) \qquad (47)$$

Balancing confining entropy of counterions with the elastic energy of the corona chains (eq 41), we obtain the equilibrium size of the micelle in the osmotic regime:

$$R_{\text{corona}} \approx bNf^{1/2} \qquad (48)$$

It is independent of the micelle aggregation number and is on the order of the corona size (eq 42) at the crossover boundary between the polyelectrolyte and osmotic regimes. The tension blob size in the osmotic regime does not depend on the aggregation number and corresponds to one charge per blob:

$$\xi_{\text{t}} \approx bf^{-1/2} \qquad (49)$$

The aggregation number in this regime is calculated by equating the surface energy of the core (eq 31) and the osmotic term of the free energy (eq (47) which leads to

$$p_{\text{osm}} \approx \frac{1}{N\left(\frac{\Delta N}{N}\right)^3 f^3}(uf^2)^{4/3} \approx \frac{1}{Z_{\text{net}}^3}\left(\frac{N}{N_{\text{neutr}}}\right)^2 \qquad (50)$$

At the crossover boundary between the polyelectrolyte and osmotic regimes the two free energy contributions $F_{\text{el}}^{\text{corona}}$ (eq 44) and F_{osm} (eq 47) are on the same order of magnitude, and the micelle aggregation numbers, given by eqs 45 and 50, are equal to each other resulting in an expression for the crossover boundary

$$Z_{\text{osm}} \approx \frac{N^{1/2}}{f^{5/4}}(uf^2)^{7/6} \qquad (51)$$

The starlike osmotic micelles remain stable even if the net charge of a block polyampholyte is as low as one elementary charge (see the horizontal thick solid line in Figure 6). This remarkable stability is due to the partitioning of the chains and can be explained by the fact that even in this limiting case the optimal micelle is starlike. Indeed, in the case of $Z_{\text{net}} = 1$ (see Figure 7), the partition is realized in such a way that there are Nf chains confined in the core (one such confined chain is shown in Figure 7) per each chain in the corona (because from eq 36 $p/p' = Nf$). In the scaling description, the condition for micelle stability is fulfilled if the number of blobs per chain in the corona $N/g_{\text{t}} \approx Nb^2/\xi_{\text{t}}^2 \approx Nf$ (see eq 49 and shaded string of blobs in Figure 7) is equal to the number of blobs per chain on the surface (see the shaded surface area in Figure 7). The total number of blobs in the core (per chain in the corona) is

$$\frac{p}{p'}\frac{N}{g} \approx Nf\frac{N}{g} \approx Nf\frac{Nb^2}{\xi^2} \approx N^2f(uf^2)^{2/3} \qquad (52)$$

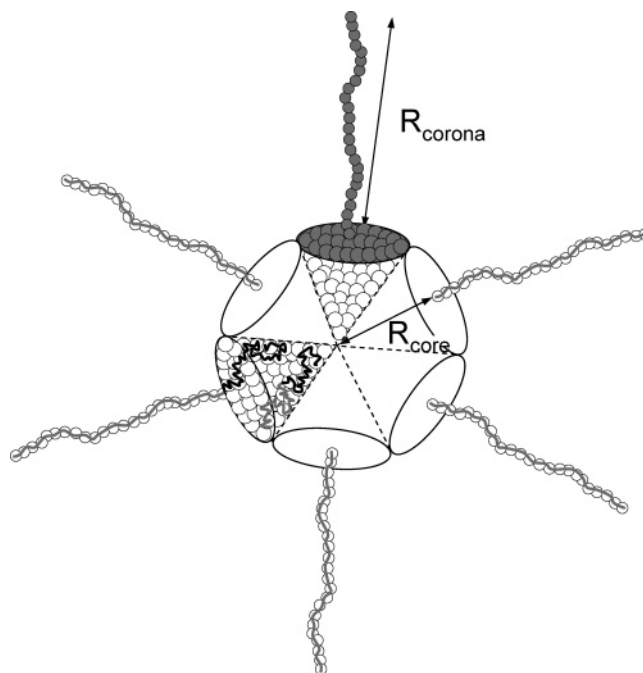Therefore, the number of blobs along the radius of the core is equal to $N(uf^2)^{2/3}$. The radius of the core is

Figure 7. Schematic sketch of chain arrangement in the starlike osmotic micelle of aggregation number p in the case of $Z_{\text{net}} = 1$. The number of chains in the corona is $p' \approx p/(Nf) \ll p$. The number of blobs in the shaded areas is equal to Nf.

estimated as

$$R_{\text{core}} \approx N(uf^2)^{2/3}\xi \approx bN(uf^2)^{1/3} \qquad (53)$$

and the radius of the corona

$$R_{\text{corona}} \approx Nf\xi_{\text{t}} \approx bNf^{1/2} \qquad (54)$$

The ratio of the two micellar dimensions

$$R_{\text{core}}/R_{\text{corona}} \approx \xi_{\text{t}}/\xi < 1 \qquad (55)$$

This inequality shows that the thickness of the corona is larger than the radius of the core and the micelle is starlike. This provides more volume per counterion confined in the micelle compared to the volume that would be available in the sediment. In the restricted model, chains are not disproportionated, so that only a section ΔN of each chain is placed in the corona. As the net charge eZ_{net} is decreased, the thickness of the corona, $R_{\text{corona}} \approx b\Delta Nf^{1/2} \approx bZ_{\text{net}}f^{-1/2}$, becomes smaller than the size of the core ($R_{\text{corona}} \ll R_{\text{core}}$). In this case counterions are mostly confined inside the core and have approximately the same entropy as in the sediment. Therefore, the restricted model without disproportionation predicts that a solution of osmotic crew-cut micelles with $R_{\text{corona}} \gg R_{\text{core}}$ phase separates even for $Z_{\text{net}} \gg 1$. Disproportionation allows osmotic micelles with small Z_{net} to become starlike ($R_{\text{corona}} \geq R_{\text{core}}$) and their solution to remain stable all the way down to $Z_{\text{net}} \approx 1$.

3.3. "Crew-Cut" Polyelectrolyte Micelles. If the radius of the core of a starlike polyelectrolyte micelle (eq 30) becomes equal to the thickness of the corona (eq 42), the crossover between the regimes of hairy and crew-cut polyelectrolyte micelles takes place:

$$Z_{\text{C-C}} \approx \frac{f}{N}(uf^2)^{-4/3} \approx Nf\left(\frac{N_{\text{neutr}}}{N}\right)^2 \qquad (56)$$

Table 1. Characteristics of the Micelles in Different Regimes from the Diagram in Figure 6

regime	D–T	star PE	star Osm	C–C PE
p	$(N^2 f^3/Z_{net}^3)(uf^2)^{-2/3}$	$(N^{4/3} f^{5/3}/Z_{net}^{5/3})(uf^2)^{-2/9}$	$(N^2/Z_{net}^3)(uf^2)^{4/3}$	$(Nf^2/Z_{net}^2)(uf^2)^{-2/3}$
R_{corona}	$[b(Nf)^2/Z_{net}^2](uf^2)^{-1/3}$	$(bN^{10/9} f^{2/9}/Z_{net}^{2/9})(uf^2)^{7/27}$	$bNf^{1/2}$	$(bNf^{1/3}/Z_{net}^{1/3})(uf^2)^{1/9}$
R_{core}	$(bNf/Z_{net})(uf^2)^{-1/3}$	$(bN^{7/9} f^{5/9}/Z_{net}^{5/9})(uf^2)^{-5/27}$	$(bN/Z_{net})(uf^2)^{1/3}$	$[b(Nf)^{2/3}/Z_{net}^{2/3}](uf^2)^{-1/3}$

Table 2. Characteristics of the Micelles in Different Regimes for the Case of an Athermal Solvent

regime	D–T	star PE	star Osm	C–C PE
p	$(N^2 f^3/Z_{net}^3)(uf^2)^{-5/7}$	$(N^{9/22} f^{8/11}/Z_{net}^{8/11})(uf^2)^{-5/22}$	$(N^2/Z_{net}^3)(uf^2)^{10/7}$	$(Nf^2/Z_{net}^2)(uf^2)^{-5/7}$
R_{corona}	$[b(Nf)^2/Z_{net}^2](uf^2)^{-3/7}$	$(bN^{12/11} f^{2/11}/Z_{net}^{2/11})(uf^2)^{12/77}$	$bNf^{2/5}$	$(bNf^{2/7}/Z_{net}^{2/7})(uf^2)^{4/49}$
R_{core}	$(bNf/Z_{net})(uf^2)^{-3/7}$	$(bN^{17/22} f^{6/11}/Z_{net}^{6/11})(uf^2)^{-41/54}$	$(bN/Z_{net})(uf^2)^{2/7}$	$[b(Nf)^{2/3}/Z_{net}^{2/3}](uf^2)^{-3/7}$

For a smaller net charge per chain ($Z_{net} \ll Z_{C-C}$) the core size of the crew-cut micelle is larger than the corona size (because of the large number of chains that are completely inside the core). In this case the micellar size is on the order of the core size, $R_{mic} \approx R_{core}$. The electrostatic energy per chain in the crew-cut polyelectrolyte regime is

$$\frac{F_{el}^{core}}{k_B T} \approx \frac{Z_{mic}^2 l_B}{p R_{core}} \approx p^{2/3} N^{5/3}\left(\frac{\Delta N}{N}\right)^2 (uf^2)^{10/9} \approx$$
$$p^{2/3} \frac{Z_{net}^2}{(Nf)^2}\left(\frac{N}{N_{neutr}}\right)^{5/3} \quad (57)$$

The aggregation number of such micelles is determined by minimizing the sum of the electrostatic energy (eq 57) and the surface energy per chain (eq 31) with respect to micellar aggregation number

$$p_{C-C} \approx \frac{1}{N\left(\frac{\Delta N}{N}\right)^2}(uf^2)^{-2/3} \approx \frac{(Nf)^2}{Z_{net}^2}\frac{N_{neutr}}{N} \quad (58)$$

This regime is denoted by "C–C PE" in the diagram in Figure 6. The electrostatic potential of these micelles is smaller than $k_B T$, and therefore their counterions remain free in solution and these crew-cut micelles are in the polyelectrolyte regime.

All micellar cores considered in the framework of the unrestricted model have spherical geometry. For the morphological transitions to other geometries (cylindrical micelles or bilayers) to occur, the core blocks have to be strongly stretched. Since the chains in the micelle are disproportionated between the core and corona, the core blocks are not stretched because most of the chains are completely confined in the core and therefore not deformed. This implies that the shape transitions do not take place for disproportionated block polyampholyte micelles.

In the restricted model, however, all chains in the core are grafted onto the core surface. Therefore, as the aggregation number is increased, the chains in the core become stretched. If the stretching energy of a chain is on the order of the difference between corona and surface free energy per chain, the spherical geometry of the core is unfavorable with respect to others (cylindrical and planar geometries).[19] Moreover, the restricted model without disproportionation predicts that the electrostatic potential of a micelle increases as the net charge per chain is decreased in the crew-cut polyelectrolyte regime (because the potential $pZ_{net}l_B/R_{mic} \sim Z_{net}^{-1/3}$, see Table 1). When the value of the potential reaches $k_B T$, the counterions begin to condense into the micelle. However, the contribution to the free energy

due to the entropy of a counterion in the core is proportional to $\ln(c_{mic})$ and does not depend on the aggregation number p. (It is clearly seen from eq 30 that the core volume, R_{core}^3, is proportional to p.) Therefore, the restricted model predicts that a macroscopic aggregate appears, and the solution phase separates into a dense sediment and a dilute supernatant. In contrast to this expectation, the unrestricted model predicts a stable solution of micelles with disproportionated chains at the same set of parameters. In fact, it predicts phase separation only for solution of charge-symmetric block polyampholytes.

3.4. Micellar Properties. In Table 1 we compile the characteristics of the four different micellar structures for the unrestricted model. The aggregation number, p, and the micellar sizes R_{corona} and R_{core} are calculated as functions of molecular parameters, such as the polymerization degree, N, the net valence per chain, Z_{net}, and the fraction of charged monomers in each block, f. The same characteristics for the case of athermal solvent are reported in Table 2. The two cases of polymer–solvent interaction are qualitatively similar but have quantitatively different power-law dependencies.

Figure 8a,b presents the dependences of the micellar aggregation number p and the size R_{mic} on the net valence per chain Z_{net} for micelles formed by block polyampholytes with a low fraction of charged monomers on each block, $f < f_w = N^{-3/5}u^{-4/5}$ (see the diagram in Figure 6). With increasing net charge one consequently crosses the regimes of solutions of crew-cut polyelectrolyte micelles, starlike polyelectrolyte micelles, and double-tailed micelles, and, at very large Z_{net}, solutions of tadpoles. Note that the regime of double-tailed micelles is very narrow and is hard to observe experimentally at low charge fractions ($f < f_w$). Both the aggregation number and the micellar size are decreasing functions of the net valence of a chain Z_{net} (except for the unimer regime). In Figure 9 the same micellar parameters are plotted for a block polyampholyte with strongly charged blocks, $f > f_s = N^{-6/13}u^{-14/13}$. Here, the regime of starlike osmotic micelles is followed by the regimes of starlike polyelectrolyte and double-tailed micelles and, at very large Z_{net}, by the regime of tadpoles. For higher charge fractions ($f > f_s$) the regime of double-tailed micelles is wider and is expected to be easier to observe. In contrast to the size of all micelles, the size of the tadpole tail increases with charge asymmetry. By comparing Figures 8 and 9, one can see that at a given net charge per chain the micelles made of block polyampholyte with strongly charged blocks are larger than those with weakly charged blocks due to a stronger attraction between oppositely charged blocks. The larger charge on the corona chains leading to the counterion confinement within micelles is the reason
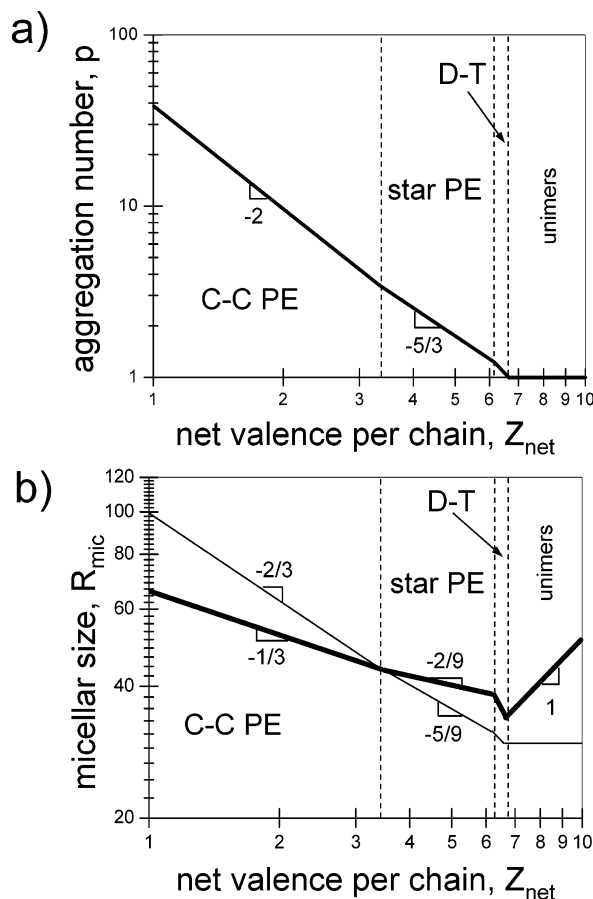
a)

b)

Figure 8. (a) Aggregation number, p, and (b) the corona thickness, R_{corona} (thick solid line), and the core size, R_{core} (thin solid line), plotted as a function of net valence per chain, Z_{net}. The radius of the head and the length of the tail of a tadpole are shown in the region marked as unimers. The plots are done for $u = 1$, $N = 1000$, and $f = 0.0075$ corresponding to weakly charged chains ($f < f_w$, see Figure 6) (logarithmic scales).

why starlike osmotic micelles are predicted for large f and crew-cut polyelectrolyte micelles are expected only for small f.

4. Discussion and Conclusions

In the present paper we have considered the equilibrium structure of a salt-free solutions of diblock polyampholytes. The oppositely charged blocks are electrostatically attracted to each other via the charge density fluctuation-induced attraction.[10] The length scale of the fluctuations, ξ, is defined by the balance between Coulomb attraction and short-range monomeric repulsion (three-body repulsion in the case of a θ-solvent) so that at this length scale the energy of both attractive and repulsive interactions are on the order of k_BT. The correlation length ξ for block polyampholytes is on the same order of magnitude as the electrostatic blob size which was defined to describe the conformation of an individual polyelectrolyte chain.[15,16] In our study the two blocks of a polyampholyte were assumed to have the same fraction of charged monomers. The nonzero net charge of the molecule is therefore proportional to the difference in the degree of polymerization of the two blocks. This uncompensated charge leads to the repulsion between the chains that stabilizes molecular aggregates.

The attraction within a chain results in a tadpole conformation of an isolated polyampholyte with a
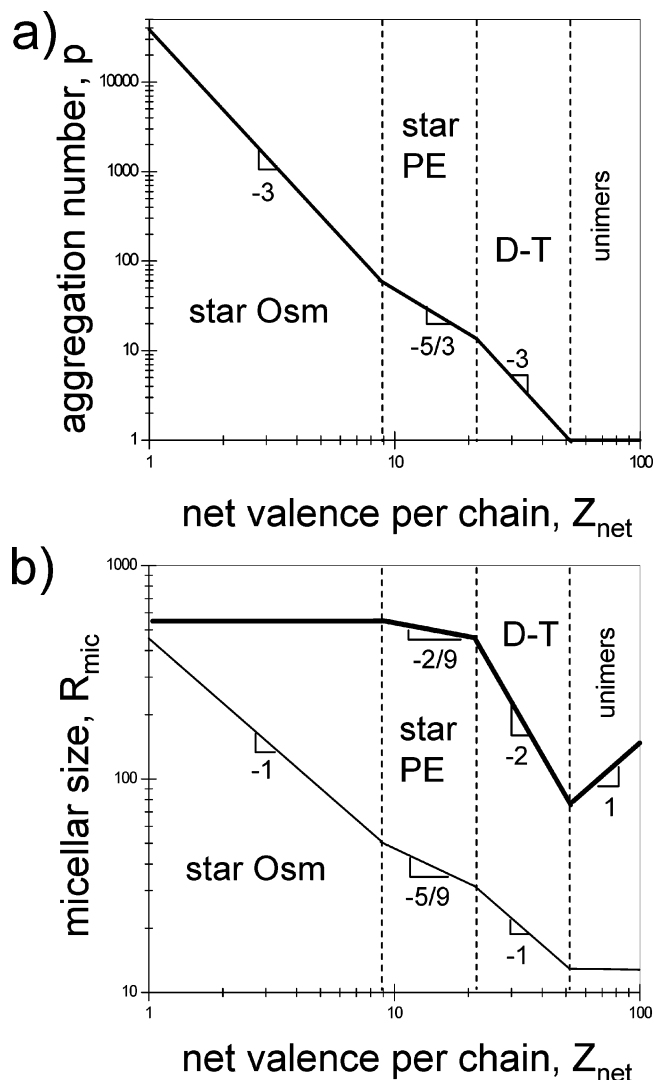
a)

b)

Figure 9. Same plots as in Figure 8 for strongly charged chains $f = 0.3$ corresponding to $f > f_s$ in Figure 6.

globular head and a polyelectrolyte tail. Two tadpoles can lower their surface energy by coalescence, but bringing together two tails increases their electrostatic repulsion. The tadpole aggregation is favorable when the surface energy of the heads dominates over the repulsion energy of the tails.

Chains partition (disproportionate) between the core and the corona of a micelles containing three, four, and more polymers. In double-tailed micelles all but two chains are completely confined into the core, and the length of the tails of the two remaining chains increases proportionally to the total charge of the micelle. When the charge of the micelle becomes higher than the charge of two corona blocks, larger micelles with starlike corona are formed. The chains in all micelles are disproportionated; they are divided into two populations—one group of chains is completely confined inside the core while another group places higher charged blocks completely in the corona.

The properties of starlike micelles of diblock polyampholytes in solution of high ionic strength have been recently described by Castelnovo and Joanny.[9] The attractive interaction in the micellar core calculated by these authors is of the same origin as considered in the present work. In their restricted model the neutral core is stabilized by short-range repulsive (screened

Coulomb) interactions in the corona. The micelles are built in such a way that all chains are in a similar conformation with the same fraction of longer blocks forming the corona. Thus, the number of blocks in the corona is equal to the total number of chains in the micelle. We have compared both micellization models and showed that the unrestricted model with disproportionation between chain conformations results in micelles with a lower free energy per chain.

The disproportionation of chains in a micelle results not only in larger aggregation numbers as compared to the case of equally distributed chains but also in enhanced stability of the homogeneous solution. Specifically, micelles formed by chains carrying the minimal possible net charge ($Z_{net} = 1$) do not precipitate but are predicted to be soluble at any solution concentration. The charged unimers aggregate into crew-cut polyelectrolyte micelles or starlike osmotic micelles depending on the fraction of charged monomers in the blocks, f. The crew-cut polyelectrolyte micelles remain soluble even in the case of minimal net charge per chain because free diblocks in the core prevent the diblocks grafted onto the core surface from being stretched. The stability of starlike osmotic micelles at $Z_{net} = 1$ is justified by the fact that the corona chains are longer than the radius of the core, so that counterions prefer to be confined to the soluble micelle rather than in the sediment. If all chains in a micelle would have a similar conformation, only a small section of each chain carrying the net charge would be placed in the corona. In this restricted model the corona is predicted to become shorter than the core radius with decreasing net charge of the chain, and the solution is predicted to phase separate. The unrestricted model proposed in the present paper predicts that charge-asymmetric block polyampholytes would not phase separate, but rather form micelles with disproportionated chains.

Let us comment on the applicability and possible extension of the model. The theory developed in the present paper is applicable to the case of monodisperse charge distribution, i.e., if all chains carry the same net charge. Charge polydispersity will shift the region of stability of a homogeneous solution. For example, the situation with an average of one elementary charge per chain can be realized by mixing positively charged, negatively charged, and uncharged chains. In this case neutral and mutually neutralized fraction would precipitate, and only the fraction carrying the total net polymer charge will remain in soluble micelles.

The scaling model described in the present paper corresponds to the case of a θ-solvent and can easily be extended to the case of a good solvent. We have reported the main results for athermal micellar solution in Table 2.

Experiments on solutions of charged polymers are always performed with a certain amount of low molecular weight salt. The addition of salt leads to screening of electrostatic interactions in the corona of starlike micelles which influences solution properties. Our model developed for a salt-free solution remains applicable for solutions of low ionic strength. The limit of applicability of the proposed model is defined by the condition $r_D \approx R_{mic}$, where r_D is the Debye screening length

$$r_D \approx b(c_s b^3 u)^{-1/2} \qquad (59)$$

and R_{mic} is the micellar size (see Table 1). The structure of coronas of starlike micelles with partially screened interactions between arms has been analyzed in refs 20 and 21. At very high ionic strength one reaches the limit considered within the restricted model by Castelnovo and Joanny[9] where the interactions in the corona are quasi-short-range being controlled by screened Coulomb potential. We expect that even in this case the chains in a micelle would still be disproportionated. The division of the chains into two groups leads to fewer chains in the corona as compared to the case of equal chain distribution and corresponding to lower micellar free energy.

In the present paper we consider the case of strong polyelectrolytes with quenched charges. In most experiments[7,8,22,23] weak polyacid−polybase block polyampholytes have been studied. The degree of dissociation of weak polyelectrolytes depends on solution pH. At a given solution pH the block charge asymmetry is defined by the difference ($N_+ f_+ - N_- f_-$). Soluble micelles can be observed if this difference is nonzero; otherwise, the solution of block polyampholytes phase separates. The case considered in this paper ($f_+ = f_-$) is realized at one particular pH if the lengths of the blocks are slightly different. At other pH values off the isoelectric point the degree of dissociation of the two blocks would be essentially different and local electrostatic potential does not modify pK of charged groups. The structure of a unimer of such a diblock polyampholyte will not be the same as considered in section 2. The scale of attractive interactions is no longer defined by eq 3 since the size of the electrostatic blobs of the two blocks are not equal. The structure of a globule is determined by fluctuations of one longer weaker charged block in the electric field of the shorter stronger charged block.[24]

The intrinsic stiffness of the blocks would dramatically change the structure of the collapsed state. Instead of dense packing of correlation blobs providing a uniform density of the globule, stiff block polyampholytes would create bundles (or tori) the formation of which is determined by competition between elastic, steric, and electrostatic interactions.

Appendix

In this appendix we derive the condition that determines the partitioning of monomers between the head and the tail of a tadpole. The partitioning of positively charged monomers between the head and the tail is determined by the balance of the fluctuation-induced attractive interaction inside the head (energy gain due to bringing an extra charge into the head) and the electrostatic potential of a positively charged monomer inside the tadpole head due to head charging (work performed upon bringing an extra charge into the head).

Consider a tadpole with the head formed by $2N_-$ charged monomers (all monomers of a negatively charged block and an equal amount of monomers of a positively charged block) and by additional N_h positively charged monomers. The condition of monomer conservation requires that $N_+ - N_- - N_h$ monomers are in the tail

of the tadpole. The free energy of the tadpole is

$$F_{\text{tadpole}} = F_{\text{head}} + F_{\text{tail}} \qquad (60)$$

The first term in eq 60 is the energy of the head consisting of the fluctuation-induced attraction (eq 10), the surface free energy of the head (eq 11), and the electrostatic self-energy of the head with charge $eZ_{\text{head}} \approx ef N_{\text{h}}$

$$\frac{F_{\text{head}}}{k_{\text{B}}T} \approx -(2N_- + N_{\text{h}})(uf^2)^{2/3} + (2N_- + N_{\text{h}})^{2/3}(uf^2)^{4/9} +$$

$$\frac{(uf^2)^{10/9}N_{\text{h}}{}^2}{(2N_- + N_{\text{h}})^{1/3}} \quad (61)$$

The free energy of the tail has the same form as that of a polyelectrolyte chain with $N_+ - N_- - N_{\text{h}}$ monomers

$$\frac{F_{\text{tail}}}{k_{\text{B}}T} \approx (N_+ - N_- - N_{\text{h}})(uf^2)^{2/3} \qquad (62)$$

In this approximation we did not take into account the electrostatic interaction between the overcharged head and tail of the tadpole. The contribution of this interaction energy to the tadpole free energy is small in comparison with either the electrostatic self-energy of the head in the case of small charge asymmetry or with the electrostatic energy of the tail in the case of highly charge-asymmetric block polyampholytes. The equilibrium partitioning of positively charged monomers between the head and tail of a tadpole is obtained by minimizing the tadpole free energy with respect to the number of the excess positively charged monomers N_{h} in the head of the tadpole

$$\frac{1}{k_{\text{B}}T}\frac{\partial F_{\text{tadpole}}}{\partial N_{\text{h}}} \approx -(uf^2)^{2/3} + \frac{(uf^2)^{4/9}}{(2N_- + N_{\text{h}})^{1/3}} +$$

$$\frac{(uf^2)^{10/9}N_{\text{h}}}{(2N_- + N_{\text{h}})^{1/3}} - \frac{(uf^2)^{10/9}N_{\text{h}}{}^2}{(2N_- + N_{\text{h}})^{4/3}} - (uf^2)^{2/3} \quad (63)$$

In the case of weak overcharging $N_{\text{h}}/N_- \ll 1$ the solution of the equation $\partial F_{\text{tadpole}}/\partial N_{\text{h}} = 0$ for the excess number of positively charged monomers N_{h} is approximated as

$$N_{\text{h}} \approx N_-{}^{1/3}(uf^2)^{-4/9} \approx N^{1/3}(uf^2)^{-4/9}\left(1 - \frac{\Delta N}{N}\right)^{1/3} \quad (64)$$

Thus, there is a weak disbalance between the number of positively and negatively charged monomers within the head of the tadpole.

The number of monomers in a tail is proportional to $\Delta N - N_{\text{h}}$. For a tail to exist this value should be positive. The crossover to the tadpole regime occurs therefore at net valence per chain

$$Z_{\text{net}} \approx N^{1/3}f(uf^2)^{-4/9} \qquad (65)$$

This boundary coincides with the one obtained using the condition of equal electrostatic potentials of the head and the tail of a tadpole (see eq 18).

References and Notes

(1) Forster, S.; Schmidt, M. *Adv. Polym. Sci.* **1995**, *120*, 51.
(2) Barrat, J.-L.; Joanny, J.-F. *Adv. Chem. Phys.* **1996**, *94*, 1.
(3) Dobrynin, A. V.; Colby, R. H.; Rubinstein, M. *J. Polym. Sci., Part B: Polym. Phys.* **2004**, *42*, 3513.
(4) Rühe, J.; Ballauff, M.; Biesalski, M.; Dziezok, P.; Gröhn, F.; Johannsmann, D.; Houbenov, N.; Hugenberg, N.; Konradi, R.; Minko, S.; Motornov, M.; Netz, R. R.; Schmidt, M.; Seidel, C.; Stamm, M.; Stephan, T.; Usov, D.; Zhang, H. *Adv. Polym. Sci.* **2004**, *165*, 79.
(5) Lowe, A. B.; McCormick, C. L. *Chem. Rev.* **2002**, *102*, 4177.
(6) Kudaibergenov, S. E. *Adv. Polym. Sci.* **1999**, *144*, 115.
(7) Goloub, T.; de Keizer, A.; Cohen Stuart, M. A. *Macromolecules* **1999**, *32*, 8441.
(8) Gohy, J. F.; Creutz, S.; Garcia, M.; Mahltig, B.; Stamm, M.; Jerome, R. *Macromolecules* **2000**, *33*, 6378.
(9) Castelnovo, M.; Joanny, J. F. *Macromolecules* **2002**, *35*, 4531.
(10) Borue, V. Y.; Erukhimovich, I. Y. *Macromolecules* **1990**, *23*, 3625.
(11) Castelnovo, M.; Joanny, J. F. *Eur. Phys. J. E* **2001**, *6*, 377.
(12) Shusharina, N. P.; Linse, P. *Eur. Phys. J. E* **2001**, *6*, 147. Shusharina, N. P.; Linse, P. *Eur. Phys. J. E* **2001**, *4*, 399.
(13) Akinchina, A.; Shusharina, N. P.; Linse, P. *Langmuir* **2004**, *20*, 10351.
(14) Zhang, R.; Shklovskii, B. T. *Physica A* **2005**, *352*, 216.
(15) de Gennes, P. G.; Pincus, P.; Velasco, R. M.; Brochard, F. *J. Phys. (Paris)* **1976**, *37*, 1461.
(16) de Gennes, P.-G. *Scaling Concepts in Polymer Physics*; Cornel University Press: Ithaca, NY, 1979.
(17) Rubinstein, M.; Colby, R. H. *Polymer Physics*; Oxford University Press: New York, 2003.
(18) Shusharina, N. P.; Nyrkova, I. A.; Khokhlov, A. R. *Macromolecules* **1996**, *29*, 3167. Shusharina, N. P.; Linse, P.; Khokhlov, A. R. *Macromolecules* **2000**, *33*, 3892.
(19) Zhulina, E. B.; Adam, M.; LaRue, I.; Sheiko, S. S.; Rubinstein, M. *Macromolecules* **2005**, *38*, 5330.
(20) Borisov, O. V.; Zhulina, E. B. *Eur. Phys. J. B* **1998**, *4*, 205.
(21) Borisov, O. V.; Zhulina, E. B. *Macromolecules* **2002**, *35*, 4472.
(22) Hadjikallis, G.; Hadjiyannakou, S. C.; Vamvakaki, M.; Patrickios, C. S. *Polymer* **2002**, *43*, 7269.
(23) Liu, S.; Armes, S. P. *Angew. Chem., Int. Ed.* **2002**, *41*, 1413.
(24) Dobrynin, O. V.; Deshkovski, A.; Rubinstein, M. *Macromolecules* **2001**, *34*, 3421.